Journal of Nuclear Medicine, published on December 20, 2019 as doi:10.2967/jnumed.119.236265

TITLE: ^{177}Lu-NM600 targeted radionuclide therapy extends survival in syngeneic murine models of triple-negative breast cancer.

RUNNING TITLE: TRT of triple-negative breast cancer

Reinier Hernandez[1,*], Joseph J. Grudzinski[1], Eduardo Aluicio-Sarduy[2], Christopher F. Massey[1], Anatoly N. Pinchuk[1], Ariana N. Bitton[1], Ravi Patel[3], Ray Zhang[1], Aakarsha V. Kumar[3], Gopal Iyer[3], Jonathan W. Engle[2], Jamey P. Weichert[1,4]

[1] Department of Radiology, University of Wisconsin-Madison, Madison, WI, USA

[2] Department of Medical Physics, University of Wisconsin-Madison, Madison, WI, USA

[3] Department of Human Oncology, University of Wisconsin-Madison, Madison, WI, USA

[4] UW Carbone Cancer Center, University of Wisconsin-Madison, Madison, WI, USA

* Corresponding author: Reinier Hernandez (Postdoctoral Fellow), Department of Radiology at the University of Wisconsin- Madison. 1111 Highland Ave WIMR 7148, Madison, WI 53705. Email: hernandez6@wisc.edu. Tel: (305)-321-9806

KEYWORDS

^{177}Lu-NM600, triple negative breast cancer, TNBC, targeted radionuclide therapy, theranostics.

ABSTRACT

There is a clinically unmet need for effective treatments for triple-negative breast cancer (TNBC) as it remains the most aggressive subtype of breast cancer. Herein, we demonstrate a promising strategy utilizing a tumor-targeting alkylphosphocholine (NM600) for targeted radionuclide therapy (TRT) of TNBC. **Methods:** NM600 was radiolabeled with ^{86}Y for PET imaging and ^{177}Lu for TRT. ^{86}Y-NM600 PET imaging was carried out in female Balb/C mice bearing syngeneic 4T07 (nonmetastatic) and 4T1 (metastatic) TNBC tumor grafts (n=3-5). Quantitative data derived from a region-of-interest analysis of the PET images, which was corroborated by *ex vivo* biodistribution, was employed to estimate the dosimetry of ^{177}Lu-NM600 treatments. Weight measurement, complete blood counts, and histopathology analysis were performed to determine ^{177}Lu-NM600 toxicity in naïve Balb/C administered 9.25 or 18.5 MBq. Groups of mice bearing 4T07 or 4T1 grafts (n=5-6) received excipient or 9.25 or 18.5 MBq ^{177}Lu-NM600 as a single or fractionated schedule, and tumor growth and overall survival were monitored. **Results:** Excellent tumor targeting and rapid normal tissue clearance of ^{86}Y-NM600 was noted in both 4T07 and 4T1 murine models. *Ex vivo* biodistribution corroborated the accuracy of the PET data and validated ^{86}Y-NM600 as surrogate for ^{177}Lu-NM600. ^{177}Lu-NM600 dosimetry showed absorbed doses of 2.04 ± 0.32 Gy/MBq and 1.68 ± 0.06 Gy/MBq to 4T07 and 4T1 tumors, respectively, which were larger than those delivered to liver (1.28 ± 0.09 Gy/MBq) and to bone marrow (0.31 ± 0.05 Gy/MBq). The ^{177}Lu-NM600 injected activities used for treatment were well tolerated and resulted in significant tumor growth inhibition and prolonged overall survival in both tested TNBC models. Complete response was attained in 60% of treated mice bearing 4T07 grafts. **Conclusions:** Overall, our results suggest that ^{177}Lu-NM600 TRT has potential for treatment of TNBC and merits further exploration in a clinical setting.

INTRODUCTION

Breast cancer accounted for 30% of the almost 880,000 new cancer cases in 2018 in the US (*1*). Approximately 15-20% of all cases are considered 'triple-negative' breast cancer (TNBC) because of undetectable levels of estrogen receptor (ER-), progesterone receptor (PR-), and human epidermal growth factor receptor 2 (HER-2-) protein at the time of diagnosis. The incidence of TNBC is higher in young minority women who face worse prognosis (both higher rates of early recurrence and death from their disease) than other ethnic groups (*2,3*). Inferior outcomes of TNBC are, in large part, attributable to (a) the common presence of micrometastatic disease at diagnosis and (b) the absence of efficacious, molecularly-targeted therapies such as the anti-estrogenic aromatase inhibitors for ER+ breast cancer and the HER2-directed agents such as trastuzumab for breast cancers expressing high (3+ score) levels of HER2. Therapies currently used to treat clinically occult TNBC micrometastatic disease are limited to conventional cytotoxic chemotherapies (e.g. anthracyclines, taxanes) that have modest efficacy at the expense of severe toxicities.(*4*)

Metabolically stable alkylphospholipid derivatives, including alkylphosphocholines, are structural mimics of cell membrane phospholipids that selectively accumulate in glycosphingolipids- and cholesterol-rich cellular membrane microdomains, known as lipid rafts(*5,6*). Lipid rafts, which play important roles in cancer cell proliferation, survival and metastasis, are markedly overexpressed by malignant cells compared to normal cells, constituting a promising mechanism for cancer-targeted therapies (*7-11*). Leveraging such a nearly universal, receptor-independent, targeting mechanism, we have developed several alkylphosphocholine analogs displaying selective tumor uptake and retention in a wide variety of cancer types, including breast cancer. In this study we investigated the properties of NM600, an alkylphosphocholine

analog with desirable tumor selectivity and pharmacokinetic profile for targeted radionuclide therapy (TRT) –a systemic radiotherapy approach that has succeeded clinically in treating several advanced cancers– in TNBC (*12,13*). Results show that the PET imaging agent, ^{86}Y-NM600, selectively targets murine TNBC tumors and can serve as a PET imaging surrogate to model the distribution and estimate the dosimetry of the therapeutic congener ^{177}Lu-NM600. In therapeutic studies using ^{177}Lu-NM600, 4T07 and 4T1 murine cancers were employed to investigate two clinically relevant TNBC phenotypes: locally aggressive and highly metastatic, respectively(*14*). In these models, treatment with ^{177}Lu-NM600 afforded tumor control and extended overall survival while showing a favorable dosimetry and toxicity profile that merits further exploration of this agent in human subjects.

MATERIALS AND METHODS

Radiochemistry and Stability

Yttrium-86 chloride was provided by the UW-Madison cyclotron group (*15*) and Lutetium-177 chloride was purchased from Missouri University Research Reactor (MURR). Radiolabeling of 2-(trimethylammonio)ethyl(18-(4-(2-(4,7,10-tris(carboxymethyl)-1,4,7,10-tetraazacyclododecan-1-yl)acetamido)phenyl)octadecyl) phosphate (NM600) with ^{86}Y and ^{177}Lu proceeded by mixing 185-370 MBq (5-10 mCi) of the radiometal with 55-110 nmol (50-100 µg) of NM600 in 0.5 M NaOAc buffer (pH=5.5). The reaction was then incubated at 95 °C for 30 minutes under constant shaking (500 rpm). ^{86}Y/^{177}Lu-NM600 was purified by reverse phase chromatography using Sep Pak C18 cartridges (Waters), eluted in absolute ethanol, dried under a N_2 stream, and reconstituted in “excipient” consisting of normal saline containing 0.4% v/v Tween20. Radiochemical yield was assessed by thin-layer chromatography using 50 mM

ethylenediaminetetraacetic acid (EDTA) mobile phase which moves the free radiometals with the solvent front (R_f=1) while ^{86}Y/^{177}Lu-NM600 remains at the origin (R_f=0).

Radiochemical purity and stability were determined via radio-high-performance liquid chromatography (HPLC) using a reverse-phase 250 x 3.00 mm C18 Luna 5µ 100 A column (Phenomenex) and a water:acetonitrile gradient (5% MeCN:0-2 min; 5-65% MeCN:2-30 min; 65-90% MeCN:30-35min; 90-5% MeCN: 35-45 min). To assess stability, 9.25 MBq of ^{177}Lu-NM600 was incubated at 37°C in both excipient and whole mouse serum, and samples were analyzed by HPLC after 2, 24, 48, 120, or 192 h of incubation. Serum samples were first mixed with an equal volume of MeCN to precipitate serum proteins, centrifuged, and the supernatant was injected into the HPLC system. All visible peaks were integrated to determine both initial purity and stability of ^{177}Lu-NM600.

Cell Culture and Animal Models

Murine mammary adenocarcinoma 4T1 and 4T07 cells lines which differ in their metastatic capacity but share a common origin(*14*), were obtained from ATCC. The cells were cultured in RPMI 1640 completed media supplemented with 10 % FBS and 1% penicillin/streptomycin in an incubator at 37°C and 5% CO_2 atmosphere.

All animal experiments were performed under the approval of the University of Wisconsin Institutional Animal Care and Use Committee. Tumor grafts were induced by subcutaneous injection of 5.0-7.5 × 10^5 4T1 or 4T07 cells into the right lower flank of 8-week old female Balb/C mice (Envigo). Tumor bearing mice were employed for in vivo imaging and therapy studies approximately 2 weeks after implantation, when tumor volume reached 400 mm^3.

^{86}Y-NM600 PET/CT Imaging

For noninvasive in vivo PET/CT imaging, mice (n=3) were administered (IV) 9.25 MBq (250 μCi) ^{86}Y-NM600 via lateral tail vein injection. Following isoflurane anesthesia (4% induction; 2% maintenance), mice were placed in prone position into the bore of a microPET/microCT scanner (Inveon, Siemens) and 40-80 million coincidence event static PET scans were acquired at 3, 24, 48, and 72 h post-injection of the radiotracer. CT scans were taken prior to each PET acquisition for attenuation correction and anatomical reference. List-mode PET scans were reconstructed using a three-dimensional ordered-subset expectation maximization (OSEM-3D) algorithm. Quantitative analysis of the images was performed by manually drawing volumes-of-interest over the tumor and other organs of interest, and data was reported as percent injected activity per gram of tissue (%IA/g), mean ± SD.

Ex Vivo Biodistribution

Ex vivo tissue distribution studies were performed to corroborate the accuracy of in vivo imaging quantification results and to test whether ^{86}Y-NM600 is a valid PET imaging surrogate of therapeutic ^{177}Lu-NM600. Two cohorts of mice bearing 4T07 or 4T1 subcutaneous tumor grafts were administered either 9.25 MBq ^{86}Y-NM600 or 3.7 MBq ^{177}Lu-NM600 via lateral tail vein injections, and mice were sacrificed by CO_2 asphyxiation 72 h post injection of the tracer. The tumor and other tissues including the blood, heart, liver, lungs, spleen, intestine, pancreas, stomach, bone, and muscle were collected, wet-weighed, and counted in an automatic gamma counter (Wizard 2, Perkin Elmer). Uptake in each tissue was expressed as %IA/g (mean ± SD).

Dosimetry Estimations

Imaging and biodistribution results were used in combination with a standardized MCNP-generated mouse model to estimate ^{177}Lu-NM600 dosimetry within the tumor and organs of interest (*16,17*). The average activity concentrations %IA/g(t) within the liver, spleen, kidneys,

heart, tumor, bone marrow, and whole-body at each time point were extrapolated to the masses of the organs of the mouse model to compute the total injected activity, $IA\%_{src}\ (t)$, within each source organ. Organs that were not delineated were assigned total injected activity proportional to their organ masses ($mass_{src}$) according to the following equation,

$$IA\%_{src}\ (t) = \ \%IA_{WB}(t) \cdot \frac{mass_{src}}{mass_{body}}$$

where $\%IA_{WB}(t)$ is the $\%IA$ within the whole-body at a given time point, t. A piecewise time-integral of $IA\%_{src}\ (t)$ was used to derive the cumulative activity within each source organ, $\tilde{A}_{src}$:

$$\tilde{A}_{src}=\int_0^\infty IA\%_{src}\ (t)dt$$

The standard mouse model, which defines the self-organ and cross-organ energy contributions to target tissue absorbed dose, $S(target \leftarrow src)$, converts the cumulative activity within each source organ into the ^{177}Lu-NM600 absorbed dose per injected activity (Gy/MBq$_{inj}$) within the tumor and each target organ ($\widetilde{D}_{target}$) by summing dose contributions from all of the source organs, including the target organ itself:

$$\widetilde{D}_{target} = \sum \tilde{A}_{src} \cdot S(target \leftarrow src)$$

Toxicity Evaluation

For longitudinal complete blood count (CBC) analysis, groups of naïve Balb/C mice (n=5) were bled (50 µl) weekly via tail vein nick for 6 weeks after injection of non-labeled NM600, 9.25 Mq, or 18.5 MBq ^{177}Lu-NM600. CBCs were determined with a VetScan HM5 (Abaxis) differential hematology analyzer. Following the last bleeding, mice were sacrificed, and the liver, spleen, kidneys, intestines, and femur bone were harvested, fixed in formalin, and sectioned for

hematoxylin and eosin (H&E) staining. H&E stained tissues were examined by a trained pathologist for gross pathology.

^{177}Lu-NM600 Treatment

Mice bearing either non-metastatic 4T07 or metastatic 4T1 subcutaneous tumors were employed for therapy studies when tumors reached a volume of approximately 400 mm^3. Groups of 5-10 mice were administered ^{177}Lu-NM600 at two injected activities, 9.25 MBq (250 μCi) or 18.5 MBq (500 μCi), or equal mass (2.5 μg) of non-radioactive NM600 (control), via lateral tail vein injection. Two additional groups of mice bearing the more aggressive 4T1 tumors received two ^{177}Lu-NM600 fractions (2×9.25 MBq or 18.5+9.25 MBq) ten days apart. Animal weight and tumor volume by calipers was monitored 2-3 times per week, and general well-being assessed daily by veterinarian staff. Humane end points were implemented, and animals were retired from the study if significant weight loss (more than 15% within a week or 20% total) was observed or when tumors reached 700% of the initial volume. The endpoint of the study was defined as survival at 120 days post-treatment.

Statistical Analysis

Based on our previous experience, we selected sample sizes of n=3-5 for imaging studies. All other experiments had a minimum sample size of n=5 which was enough detect an effect size of 2 in mean survival, with 90% power at 5% significance level. Statistical comparison between individual groups was performed via two-tailed student T-test with a $P < 0.05$ for statistical significance. Survival data was presented as Kaplan-Meier curves and the groups were statistically compared using log-rank test. All statistics were performed using Graphpad Prism 7 (San Diego, CA).

RESULTS

Radiochemistry and Stability

Both ^{86}Y-NM600 and ^{177}Lu-NM600 were synthesized in nearly quantitative yields (>95%) and with excellent radiochemical purities (>98%), at a similar apparent molar activity of 3.4 MBq/nmol. The stability of ^{177}Lu-NM600 in excipient and complete serum was studied by serial radio-HPLC out to 192 h post incubation. No early radiopeaks that might indicate demetallation were noted (Figure 1A) in HPLC of excipient; only a single radio-peak (Rt: 23.8 min), corresponding to ^{177}Lu-NM600 was observed. At the 192 h time point, a secondary radiopeak (Rt: 26.3 min) was observed in samples incubated in serum, which amounted to 6% of the integrated area of the main radiopeak.

PET/CT Imaging and Biodistribution

Longitudinal PET/CT studies were performed to investigate the tumor targeting and biodistribution of ^{86}Y-NM600 and to estimate the dosimetry of the ^{177}Lu-NM600 therapeutic analog in two murine models of breast cancer. Figure 2A shows maximum intensity projection (MIP) PET images of the in vivo distribution of ^{86}Y-NM600 following IV injection in balb/C mice bearing 4T07 or 4T1 tumor grafts. Quantitative region of interest analysis of the PET images (Figure 2B, C and Supplementary table 1) revealed elevated blood pool activity of the radiotracer at the early, 4 h post-injection (p.i.), timepoint which gradually declined with a 20.4 ± 4.3 h blood clearance half-life (Supplemental figure 1). Due to the hepatobiliary excretion of the agent, liver peak uptake values at 24 h p.i. were 9.3 ± 1.1 %IA/g and 11.3 ± 1.9 %IA/g in the 4T07 and 4T1 models, which gradually declined upon radiotracer excretion. Uptake in normal organs including kidneys, spleen, skeletal bones, and muscle was below 6 %IA/g at all measured timepoints. Elevated and sustained tumor accretion of ^{86}Y-NM600 was observed at 4 h p.i. and continued to

increase to peak values of 11.0 ± 1.3 %IA/g and 12.9 ± 1.3 %IA/g, in 4T1 and 4T07 tumors, respectively. Prolonged tumor retention was evidenced by a high tumor radioactivity at 72 h p.i.

Following the last imaging session at 72 h p.i. of ^{86}Y-NM600, ex vivo biodistribution studies were carried out and the result compared with similar groups of mice that received ^{177}Lu-NM600 (Figure 3 and Supplemental table 2). Excellent agreement in tumor uptake and normal tissue biodistribution was observed between ^{86}Y-NM600 and ^{177}Lu-NM600 injected at the same mass dose, which corroborated the elevated tumor accumulation and retention, and hepatobiliary clearance observed via PET/CT imaging. These results corroborated the feasibility of employing ^{86}Y as a PET imaging surrogate of ^{177}Lu, allowing for the image-based dosimetry estimation of therapeutic ^{177}Lu-NM600.

Dosimetry Estimations

Tumor and normal organ dosimetry for ^{177}Lu-NM600 in two murine tumor models of TNBC were estimated using PET/CT imaging in combination with a standardized mouse model. Figure 4 and Supplemental table 3 summarize the dosimetry results showing an absorbed dose per activity of 2.04 ± 0.32 Gy/MBq and 1.68 ± 0.06 Gy/MBq to 4T07 and 4T1 tumors, respectively. The normal organ which had the largest dose was the liver with 1.12 ± 0.09 Gy/MBq and 1.28 ± 0.09 Gy/MBq, respectively, which can be attributed to the hepatobiliary clearance of the agent. The remaining normal tissues had absorbed dose values well under 1.0 Gy/MBq, notably the bone marrow with 0.31± 0.05 Gy/MBq and 0.28 ± 0.04 Gy/MBq, respectively.

Toxicity Evaluations

A longitudinal complete blood count (CBC) analysis in naïve Balb/C mice administered ^{177}Lu-NM600 was performed to evaluate potential hematological toxicity (Figure 5A). Compared

to control mice, injection of 9.25 or 18.5 MBq ^{177}Lu-NM600 resulted in mild, dose-dependent, cytopenia. In both groups, moderate leukopenia was observed with NADIR at day 10 and resolution at weeks 4 and 5 after treatment in the 9.25 MBq and 18.5 MBq groups, respectively. Anemia was also apparent in treated mice, though to a lesser extent and with faster recovery times. No overt thrombocytopenia was noted as no significant difference in platelet levels between treated mice and controls was observed. Finally, ^{177}Lu-NM600 administration had no significant ($P > 0.05$) impact in animal weight.

Following a recovery period of 6 weeks after ^{177}Lu-NM600 administration, histological (H&E) examination of the main organs at risk for radiotoxicity including the liver, kidneys, spleen, bone marrow, and intestine showed no signs of overt tissue degeneration (Supplemental figure 2). The bone marrow presented normal cellularity even at the highest injected activity. Tubular degeneration, an indication of kidney radiotoxicity, was not observed in the kidney sections, and hepatocytes showed normal morphology. Overall, these results corroborated the tolerability of ^{177}Lu-NM600 treatment and pointed to the bone marrow as the potential dose-limiting organ.

^{177}Lu-NM600 Therapy

Three groups of mice (n = 5) bearing 4T07 tumor grafts received a single 9.25 or 18.5 MBq injection of ^{177}Lu-NM600 or equimolar amount of non-radioactive NM600. Significant tumor growth inhibition compared to controls ($P < 0.05$) was noted between days 17 and 19 in all treated cohorts (Figure 6A and Supplemental figure 3), and mice receiving 18.5 MBq achieve marked tumor regression. Such effective tumor response translated into an extended survival in both treatment cohorts (Figure 6B). In contrast with a median overall survival (OS) of 25 days for the control group, median OS was not achieved over the 100-day observation period. Additionally,

60% and 80% of mice achieved complete tumor response in the 9.25 and 18.5 MBq groups, respectively.

Consistent with its aggressive phenotype, 4T1 tumors proved difficult to cure by either single or fractionated ^{177}Lu-NM600 treatment. Local tumor control was afforded by treatment with single or fractionated ^{177}Lu-NM600 (Figure 6C and Supplemental figure 4), with the group receiving 18.5 MBq followed by 9.25 MBq, 10 days after the first dose, achieving significant regression of the primary grafts. All four treatment schedules resulted in significantly ($P< 0.0001$) prolonged survival compared to controls (Figure 6D), who quickly succumbed to primary tumor growth. Median overall survival was 8, 26, 22, 26, and 21 days in the control (n = 10), 9.25 MBq (n = 7), 18.5 MBq (n = 10), 2×9.25 MBq (n = 7), and 18.5+9.25 MBq (n = 10) groups, respectively. Despite the effective local tumor control and clear survival benefit of ^{177}Lu-NM600 treatment, no complete responses were recorded in any of the treatment arms. Necropsy in these mice revealed a prevalent metastatic burden in the lungs, this being likely the cause of animal mortality.

DISCUSSION

TRT has proven effective in patients with advanced, hormone therapy resistant, solid tumors including metastatic castration resistant prostate tumors and gastroenteropancreatic neuroendocrine tumors (*12,13,18,19*), and it is plausible that similar responses can be achieved in TNBC using tumor-selective radiolabeled agents. Therefore, we investigated the properties of ^{177}Lu-NM600 as a TRT agent for the treatment of TNBC. Leveraging the radiochemical versatility of NM600, we implemented a theranostic approach using ^{86}Y-NM600 as a PET imaging surrogate that estimated the ^{177}Lu-NM600 dosimetry and established the dose-effect relationships of the agent.

^{86}Y-NM600 was selectively retained in two murine models of TNBC. Hepatobiliary excretion of the agent was confirmed by gradual declines in liver and intestinal signals. Overall, ^{86}Y-NM600 showed a favorable tissue biodistribution suggesting the existence of a suitable therapeutic window for ^{177}Lu-NM600 TRT. Both in vivo imaging and ex vivo biodistribution studies validate the ^{86}Y-NM600 as an imaging surrogate for ^{177}Lu-NM600, permitting the estimation of ^{177}Lu-NM600 dosimetry using PET imaging.

Tumor doses in the 4T07 and 4T1 models were 1.8 and 1.3 times higher than that of the liver, the organ with the highest ^{86}Y-NM600 uptake. As predicted by image-derived dosimetry, no overt radiotoxicity was observed by histopathology in the liver, spleen, and kidneys of Balb/C mice administered up to 18.5 MBq ^{177}Lu-NM600, the equivalent to a maximum of 25 Gy, 9 Gy, and 10 Gy to the liver, spleen, and kidneys, respectively. Bone marrow on the other hand showed signs of a dose dependent radiotoxicity as evidenced by reported transient lymphopenia and anemia following 9.25 or 18.5 MBq ^{177}Lu-NM600 administration. These findings were confirmed by both CBC and histopathology analysis and suggest bone marrow as the dose limiting organ. Overall, besides mild cytopenia, ^{177}Lu-NM600 treatment was well tolerated. Absorbed dose to tumors, which were higher than any other tissue, were as high as 31 Gy and 38 Gy for a single 18.5 MBq fraction in the 4T07 and 4T1 tumors, respectively. Such elevated tumor doses resulted in effective tumor growth inhibition and prolonged overall survival in all TRT treatment arms compared to NM600 treated controls. In mice bearing 4T07 tumors, complete tumor eradication was achieved in 50% and 60% of the animals in the 9.25 MBq and 18.5 MBq cohorts, respectively. Despite showing regression of the primary grafts and extended survival, complete responses were not observed in treated mice bearing the metastatic 4T1 tumors. Use of fractionated schedule did

not provide an additional benefit in animal survival, which all succumbed to metastatic disease in the lungs.

The failure of ^{177}Lu-NM600 to completely stop metastatic progression in 4T1 mice may be ascribed to several conditions. It is likely that at the time of treatment metastatic tumor foci or large cell clusters (< 1-2 mm^3) had not formed appropriate vasculature, limiting ^{177}Lu-NM600 uptake (*20,21*). Additionally, due to the intermediate range of ^{177}Lu β- emissions (1.7 mm), even those metastatic lesions with prominent tumor uptake received a much lower radiation dose than those in a macroscopic tumor with significant cellular crossfire, resulting in tumor progression of the metastatic lesions (*22*). In follow up studies, we will investigate the ability of NM600 radiolabeled with short range, high linear energy transfer (LET), radionuclides (e.g., ^{225}Ac, ^{227}Th, ^{212}Pb), to eradicate microscopic disease. Of note, the described microdosimetric effects will be less relevant in humans subjects since metastatic breast cancer lesions tend to be much larger (> 5 mm) at diagnosis compared to those observed in mice (<1 mm) (*23*). Finally, another approach to increase the cure rate in this aggressive model will be to combine ^{177}Lu-NM600 with other systemic anti-tumor therapies such as immunotherapy or poly (adenosine diphosphate-ribose) polymerase (PARP) inhibitors, which have shown promise in those patients carrying BRCA1 and BRCA2 mutations (*12,13,18,19*). The potential of this approach was demonstrated by Filatenkov and associates(*24*) using external beam radiotherapy in combination with adoptive T-cell transplant to achieve long-term survival in the 4T1 model.

The absorbed doses based on our image-based dosimetry are likely to be underestimated due to the limitations associated with small animal PET imaging. Because positron range correction was not performed, partial volume effects may have contributed to uncertainty in the dosimetry results. For example, the relatively long positron range of ^{86}Y (mean of 3.9 mm) can

cause signal spillover into organs which are adjacent to the liver which may lead to an overestimation of activity and dose within these organs. Additionally, because of the relatively small beta energy of ^{177}Lu (average pathlength < 1 mm), there is minimal dose spillover between organs that are not in direct contact with one another. Therefore, any 'cross-fire' between organs is mainly due to partial volume effects innate to the PET imaging and not the energy of the betas. These problems associated with the image acquisition will be less relevant as we progress to human studies where the spacing between neighboring organs is larger than the positron range of ^{86}Y.

CONCLUSION

We demonstrated that ^{177}Lu-NM600 may be a promising treatment option for TNBC by extending survival in a population of patients for which effective therapies are lacking. Its favorable safety profiles and efficacy against aggressive tumor models provides motivation for continual investigation and potential clinical translation.

DISCLOSURE

R.H., J.J.G., and A.N.P are consultants to Archeus Technologies, Inc. J.P.W. is a co-founder and stockholder of Archeus Technologies, Inc. which holds the licensing rights to NM600. No other potential conflicts of interest relevant to this article exist.

ACKNOWLEDGEMENTS

We are grateful to Archeus Technologies Inc. for providing the NM600 stable precursor. We thank the efforts of the UW Small Animal Imaging Facility and support provided by the University of Wisconsin Carbone Cancer Center Support Grant (P30 CA014520 and gifts). Part of this work was supported by the National Cancer Institute of the National Institutes of Health (awards U01CA233102 and T32CA009206)

KEY POINTS

QUESTION: Is targeted radionuclide therapy a viable treatment option for triple-negative breast cancer (TNBC)?

PERTINENT FINDINGS: In two murine models of locally advanced and metastatic TNBC, respectively, we demonstrated the ability of ^{177}Lu-NM600 to selectively deliver significant radiation doses to tumors. Such high cumulative absorbed doses resulted in significant tumor control and extended survival without incurring prohibitive normal tissue toxicity.

IMPLICATIONS FOR PATIENT CARE: In this aggressive cancer type with few treatment options, ^{177}Lu-NM600 has the potential to become a clinically viable therapeutic for TNBC.

REFERENCES

1. Howlader N NA, Krapcho M, Miller D, et al (eds). *SEER Cancer Statistics Review, 1975-2016* National Cancer Institute. Bethesda, MD, https://seer.cancer.gov/csr/1975_2016/, based on November 2018 SEER data submission, posted to the SEER web site, April 2019. 2019.

2. DeSantis C, Siegel R, Bandi P, Jemal A. Breast cancer statistics, 2011. *CA Cancer J Clin.* 2011;61:409-418.

3. Giltnane JM, Balko JM. Rationale for targeting the Ras/MAPK pathway in triple-negative breast cancer. *Discov Med.* 2014;17:275-283.

4. Hudis CA, Gianni L. Triple-negative breast cancer: an unmet medical need. *Oncologist.* 2011;16 Suppl 1:1-11.

5. Vink SR, van der Luit AH, Klarenbeek JB, Verheij M, van Blitterswijk WJ. Lipid rafts and metabolic energy differentially determine uptake of anti-cancer alkylphospholipids in lymphoma versus carcinoma cells. *Biochem Pharmacol.* 2007;74:1456-1465.

6. Kaleagasioglu F, Zaharieva MM, Konstantinov SM, Berger MR. Alkylphospholipids are Signal Transduction Modulators with Potential for Anticancer Therapy. *Anticancer Agents Med Chem.* 2019;19:66-91.

7. van der Luit AH, Vink SR, Klarenbeek JB, et al. A new class of anticancer alkylphospholipids uses lipid rafts as membrane gateways to induce apoptosis in lymphoma cells. *Mol Cancer Ther.* 2007;6:2337-2345.

8. Weichert JP, Clark PA, Kandela IK, et al. Alkylphosphocholine analogs for broad-spectrum cancer imaging and therapy. *Sci Transl Med.* 2014;6:240ra275.

9. Grudzinski JJ, Hernandez R, Marsh I, et al. Preclinical Characterization of (86/90)Y-NM600 in a Variety of Murine and Human Cancer Tumor Models. *J Nucl Med.* 2019;60:1622-1628.

10. Hernandez R, Walker KL, Grudzinski JJ, et al. (90)Y-NM600 targeted radionuclide therapy induces immunologic memory in syngeneic models of T-cell Non-Hodgkin's Lymphoma. *Commun Biol.* 2019;2:79.

11. Murai T. The role of lipid rafts in cancer cell adhesion and migration. *Int J Cell Biol.* 2012;2012:763283.

12. Strosberg J, El-Haddad G, Wolin E, et al. Phase 3 Trial of (177)Lu-Dotatate for midgut neuroendocrine tumors. *N Engl J Med.* 2017;376:125-135.

13. Kratochwil C, Giesel FL, Stefanova M, et al. PSMA-Targeted Radionuclide Therapy of Metastatic Castration-Resistant Prostate Cancer with 177Lu-Labeled PSMA-617. *J Nucl Med.* 2016;57:1170-1176.

14. Heppner GH, Miller FR, Shekhar PM. Nontransgenic models of breast cancer. *Breast Cancer Res.* 2000;2:331-334.

15. Aluicio-Sarduy E, Hernandez R, Valdovinos HF, et al. Simplified and automatable radiochemical separation strategy for the production of radiopharmaceutical quality (86)Y using single column extraction chromatography. *Appl Radiat Isot.* 2018;142:28-31.

16. Beatty BG, Kuhn JA, Hui TE, Fisher DR, Williams LE, Beatty JD. Application of the cross-organ beta dose method for tissue dosimetry in tumor-bearing mice treated with a 90Y-labeled immunoconjugate. *Cancer.* 1994;73:958-965.

17. Miller WH, Hartmann-Siantar C, Fisher D, et al. Evaluation of beta-absorbed fractions in a mouse model for 90Y, 188Re, 166Ho, 149Pm, 64Cu, and 177Lu radionuclides. *Cancer Biother Radiopharm.* 2005;20:436-449.

18. Kam BL, Teunissen JJ, Krenning EP, et al. Lutetium-labelled peptides for therapy of neuroendocrine tumours. *Eur J Nucl Med Mol Imaging.* 2012;39 Suppl 1:S103-112.

19. Kratochwil C, Bruchertseifer F, Giesel FL, et al. 225Ac-PSMA-617 for PSMA-Targeted alpha-Radiation Therapy of Metastatic Castration-Resistant Prostate Cancer. *J Nucl Med.* 2016;57:1941-1944.

20. Hillen F, Griffioen AW. Tumour vascularization: sprouting angiogenesis and beyond. *Cancer Metastasis Rev.* 2007;26:489-502.

21. Nishida N, Yano H, Nishida T, Kamura T, Kojiro M. Angiogenesis in cancer. *Vasc Health Risk Manag.* 2006;2:213-219.

22. Marcu L, Bezak E, Allen BJ. Global comparison of targeted alpha vs targeted beta therapy for cancer: In vitro, in vivo and clinical trials. *Crit Rev Oncol Hematol.* 2018;123:7-20.

23. Dillekas H, Transeth M, Pilskog M, Assmus J, Straume O. Differences in metastatic patterns in relation to time between primary surgery and first relapse from breast cancer suggest synchronized growth of dormant micrometastases. *Breast Cancer Res Treat.* 2014;146:627-636.

24. Filatenkov A, Baker J, Muller AM, et al. Treatment of 4T1 metastatic breast cancer with combined hypofractionated irradiation and autologous T-cell infusion. *Radiat Res.* 2014;182:163-169.

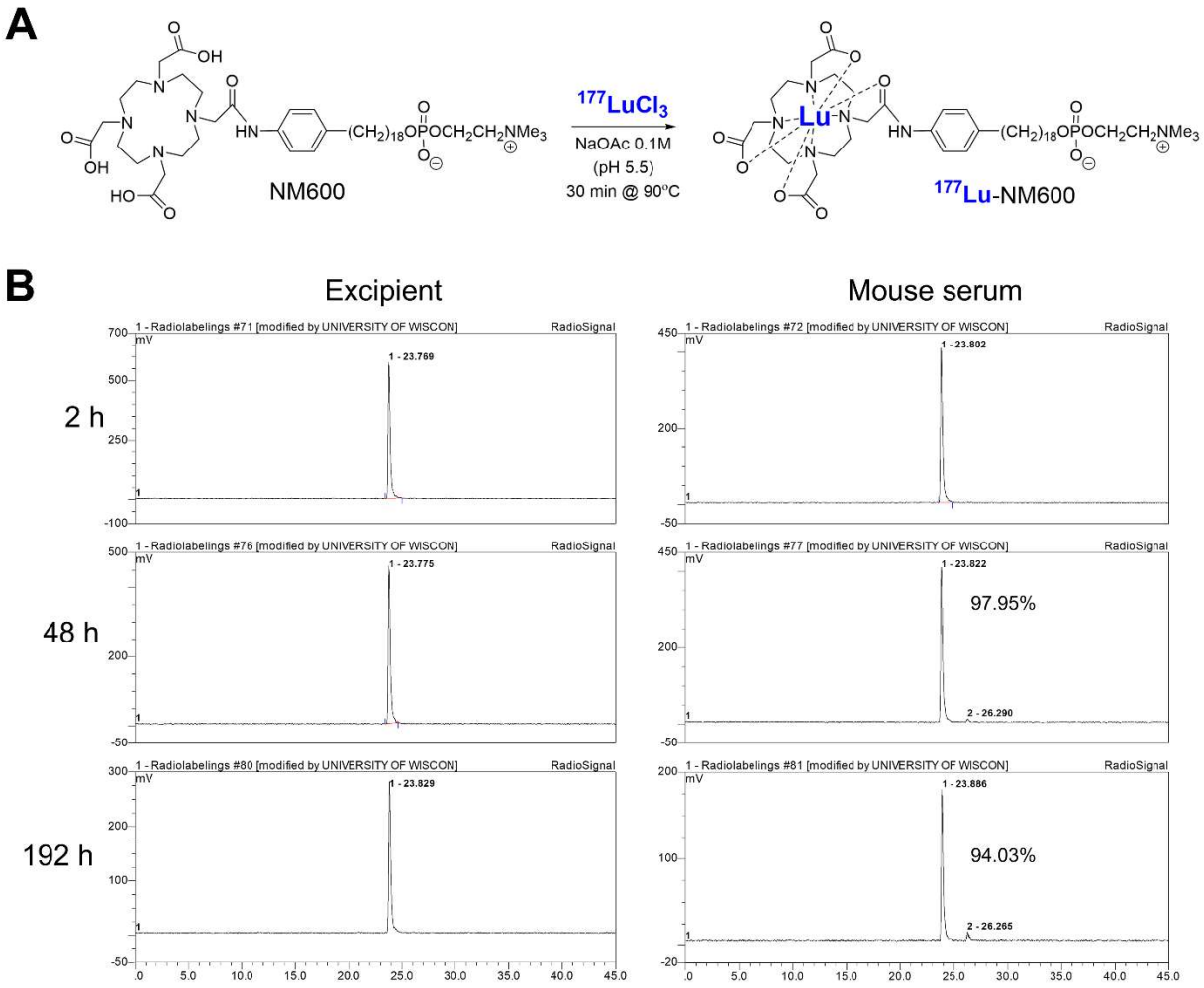

Figure 1. Radiochemical synthesis and stability of ^{177}Lu-NM600. **A)** Schematic representation of ^{177}Lu-radiolabeling of NM600. **B)** ^{177}Lu-NM600 stability was assessed in the injectable formulation and in mouse serum at 37 °C for up to 192 h. No degradation was noted when incubated in excipient. Secondary radiopeaks corresponding to impurities were observed in serum but radiochemical purity remained >94% at 192 h post incubation.

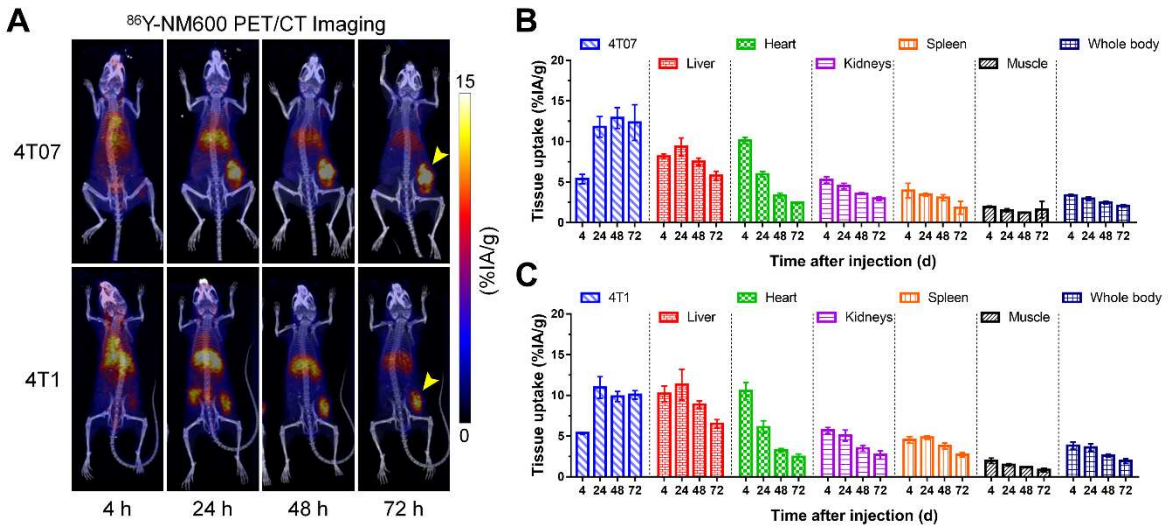

Figure 2. Longitudinal ^{86}Y-NM600 PET/CT imaging in murine models of TNBC. **A)** PET/CT maximum intensity projection images of mice bearing 4T07 or 4T1 subcutaneous grafts at 4, 24, 48 and 72 h after intravenous administration of ^{86}Y-NM600 (n=3). Elevated and persistent uptake of the radiotracer in the tumor and gradual hepatobiliary clearance were observed. Results of a quantitative region-of-interest analysis of the PET imaging in mice bearing subcutaneous 4T07 **(B)** or 4T1 **(C)** breast adenocarcinomas. Data is presented as percent injected activity per gram (%IA/g; mean ± SD).

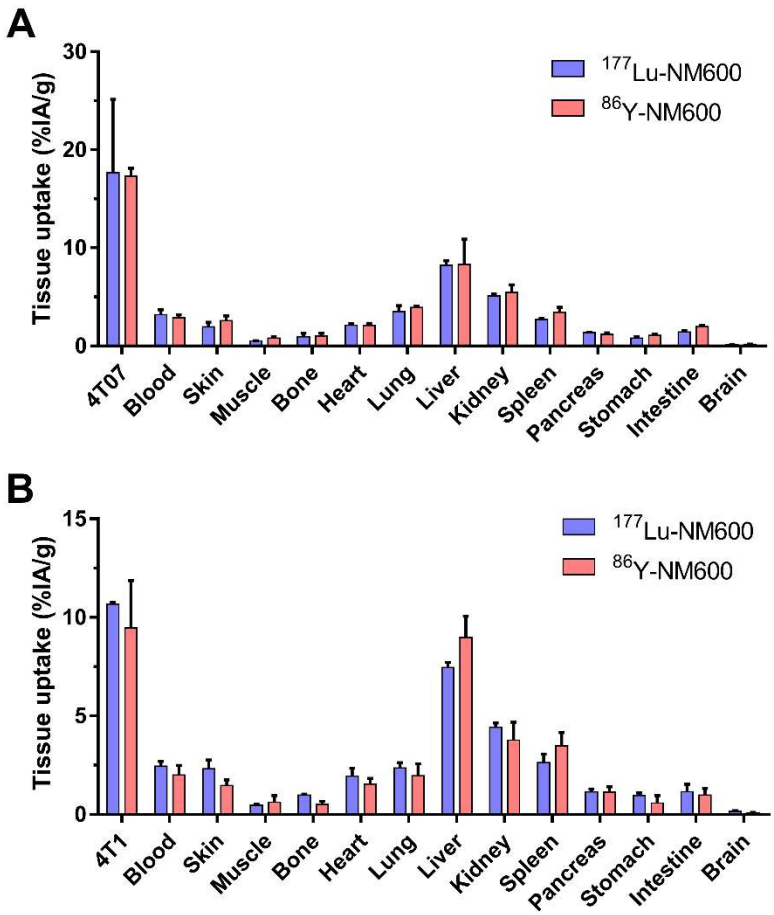

Figure 3. Ex vivo biodistribution of ^{86}Y-NM600 and ^{177}Lu-NM600, at 72 h post-injection, in mice bearing **(A)** 4T07 or **(B)** 4T1 murine breast cancer grafts. Notable agreement between the tumor uptake and normal tissue distribution of both agents was observed.

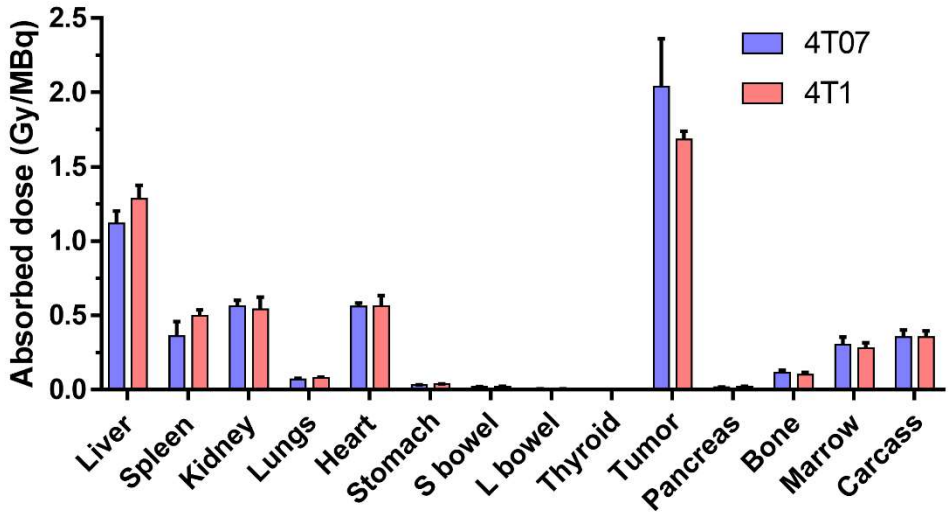

Figure 4. PET/CT imaging-based tumor and normal organ dosimetry estimation of ^{177}Lu-NM600 in Balb/C mice bearing 4T07 and 4T1 breast tumor grafts. Tumors received the highest dose of all analyzed tissues, 2.04 ± 0.32 and 1.68 ± 0.06 Gy/MBq for 4T07 and 4T1 tumors, respectively.

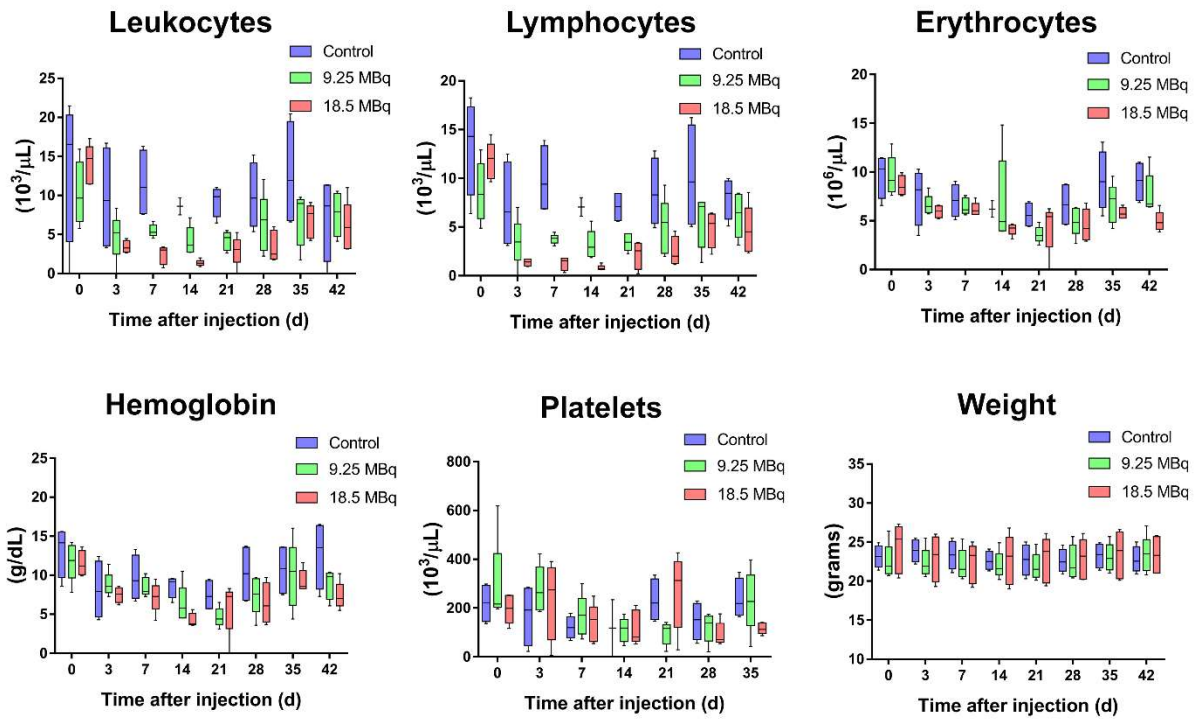

Figure 5. Longitudinal complete blood count and weight analysis in mice administered unlabeled NM600 (control), or ^{177}Lu-NM600, at a 9.25 or 18.5 MBq injected activity (n = 5). Dose dependent lymphopenia and anemia were observed in treated mice with a NADIR at 10 days post-injection of the agent and a 5-week recovery period. No mortality was reported among treated animals. No significant change in animal weight was noted compared to controls in mice treated with ^{177}Lu-NM600.

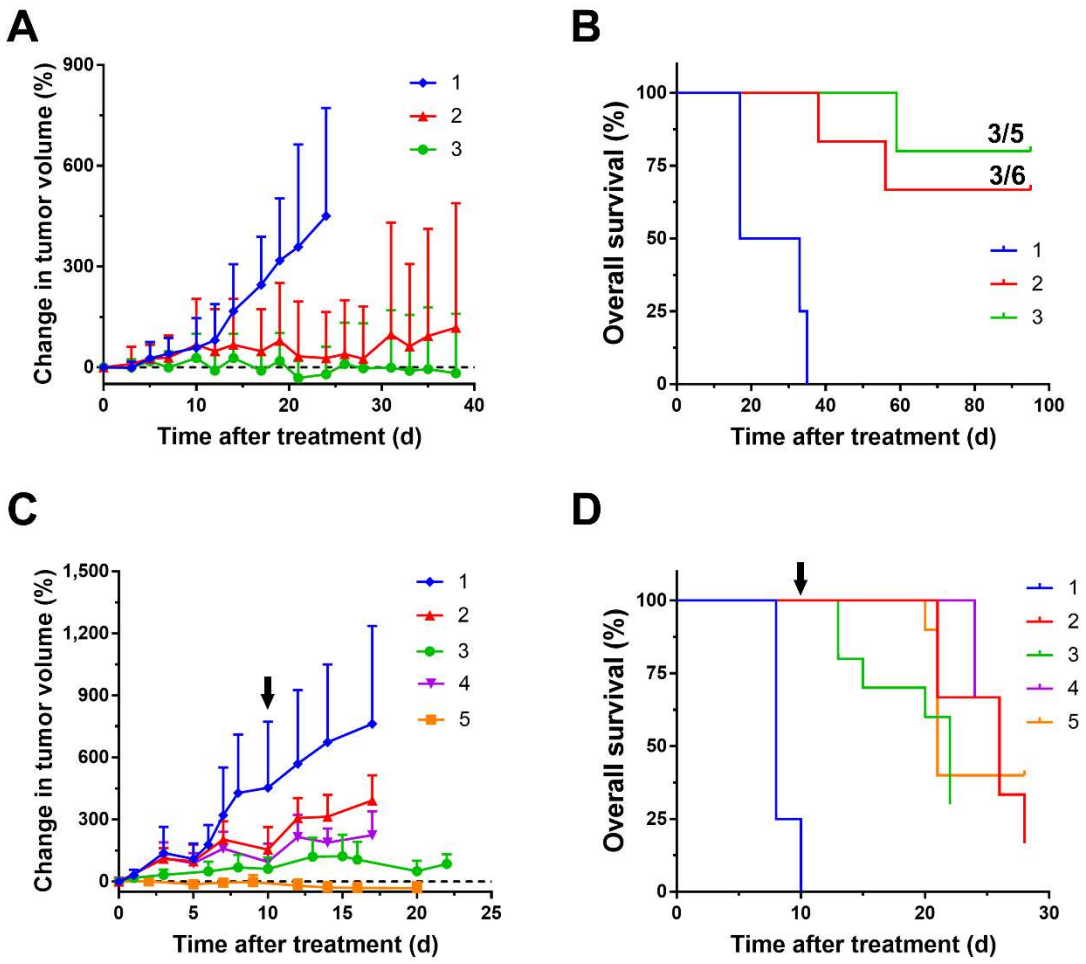

Figure 6. ^{177}Lu-NM600 treatment inhibits tumor growth and extends survival in mice bearing syngeneic TNBC grafts. Tumor growth curves **(A)** and overall survival (**B)** of mice bearing 4T07 grafts treated with increasing ^{177}Lu-NM600 injected activity. Significant tumor growth inhibition and prolonged median overall survival was noted in all treated mice. Complete response was achieved in 50% (3/6) and 60% (3/5) of mice treated with 9.25 MBq and 18.5 MBq injections, respectively. In mice bearing 4T1 tumors, administration of single (9.25 MBq or 18.5 MBq) or fractionated (2×9.25 MBq or 18.5+9.25 MBq) ^{177}Lu-NM600 resulted in significant tumor growth inhibition **(C)** and extended overall survival **(D)**, although complete responses were not attained. Black arrows denote the time of the second ^{177}Lu-NM600 injection in the fractionated treatment arms.

Table 1. Summary of the experimental conditions and results of ^{177}Lu-NM600 therapy studies.

Tumor Model	Treatment Arm	Sample Size	Injected Activity (MBq)	Tumor Absorbed Dose (Gy)	Median OS (days)
4T07	1	5	Control (0)	0	25
	2	6	9.25	18.9	N/A
	3	5	18.5	37.7	N/A
4T1	1	10	Control (0)	0	8
	2	7	9.25	15.5	26
	3	10	18.5	31.0	22
	4	7	2 × 9.25	31.0	26
	5	10	18.5 + 9.25	46.5	21

OS: Overall survival

Supplemental information

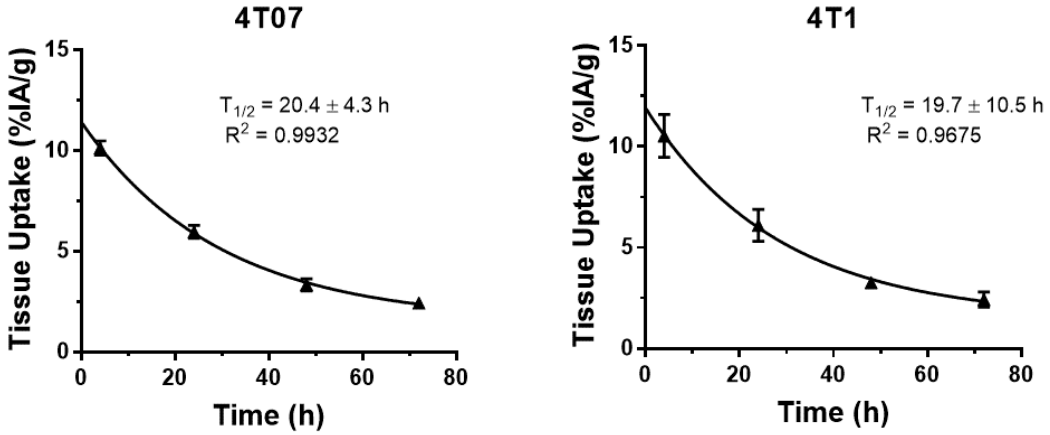

Supplemental figure 1 Blood time-activity curves of ^{86}Y-NM600 in Balb/C mice bearing syngeneic s.c. 4T07 or 4T1 breast tumors. Blood circulation half-life ($T_{1/2}$) was calculated by fitting the quantitative PET data to a monoexponential decay. Similar circulation $T_{1/2}$ were observed (20.4 ± 4.3 h vs. 19.7 ± 10.5 h) between the two groups.

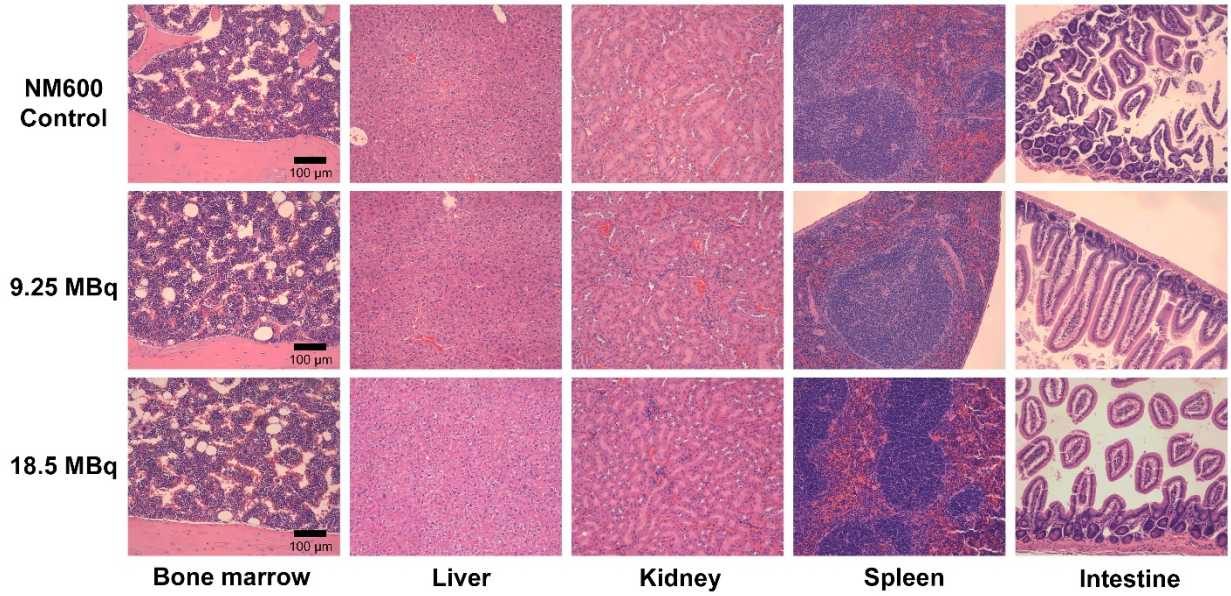

Supplemental figure 2. Histopathology examination of H&E tissue sections corresponding to the bone marrow, liver, kidney, spleen, and small intestine, six weeks after injection of NM600, or ^{177}Lu-NM600 9.25 MBq or 18.5 MBq. Similar tissue morphology was noted in all analyzed sections, indicating the absence of tissue degeneration. Scale bars represent 100 µm

Supplemental table 1 Results of the region-of-interest analysis of the longitudinal PET/CT data in mice bearing 4T1 or 4T07 subcutaneous grafts and administered ^{86}Y-NM600 (9.25 MBq). Data are presented as %IA/g (mean ± SD).

Time (h p.i.)	Tumor (%IA/g)		Heart/blood (%IA/g)		Liver (%IA/g)		Spleen (%IA/g)		Kidneys (%IA/g)		Muscle (%IA/g)		Bone/Marrow (%IA/g)		Whole Body (%IA/g)	
	Mean	**SD**	**Mean**	**SD**	**Mean**	**SD**	**Mean**	**SD**	**Mean**	**SD**	**Mean**	**SD**	**Mean**	**SD**	**Mean**	**SD**
86Y-NM600 in 4T1 bearing mice																
4	5.4	0.1	10.5	1.1	10.2	1.0	4.5	0.4	5.7	0.4	2.0	0.3	2.2	0.3	3.8	0.5
24	11.0	1.3	6.1	0.8	11.3	1.9	4.8	0.2	5.1	0.7	1.5	0.2	1.7	0.3	3.6	0.4
48	9.9	0.6	3.3	0.2	8.9	0.5	3.8	0.4	3.5	0.4	1.2	0.1	1.3	0.1	2.6	0.2
72	10.1	0.5	2.4	0.4	6.5	0.5	2.7	0.3	2.7	0.5	0.8	0.2	1.0	0.1	1.9	0.3
86Y-NM600 in 4T07 bearing mice																
4	5.4	0.6	10.1	0.4	8.2	0.3	3.9	0.9	5.3	0.4	1.9	0.1	2.2	0.1	3.4	0.1
24	11.8	1.3	6.0	0.3	9.3	1.1	3.4	0.2	4.5	0.3	1.5	0.2	1.8	0.3	3.0	0.2
48	12.9	1.3	3.3	0.3	7.5	0.5	3.1	0.4	3.6	0.1	1.2	0.1	1.4	0.3	2.5	0.2
72	12.3	2.2	2.4	0.1	5.8	0.6	1.8	0.8	3.0	0.2	1.6	1.0	1.1	0.2	2.1	0.2

Supplemental table 2 Results of *ex vivo* biodistribution in mice bearing 4T07 or 4T1 tumors grafts, and administered either 86Y-NM600 (9.25 MBq) or ^{177}Lu-NM600 (9.25 MBq), 72 h post-injection. Data is presented as %IA/g (mean ± SD).

	4T07 bearing mice				4T1 bearing mice			
Agent	86Y-NM600		^{177}Lu-NM600		86Y-NM600		^{177}Lu-NM600	
Tissue	**Mean***	**SD**	**Mean***	**SD**	**Mean***	**SD**	**Mean***	**SD**
Tumor	17.31	0.80	17.67	7.48	9.47	2.40	10.67	0.08
Blood	2.89	0.27	3.19	0.51	2.01	0.49	2.45	0.25
Skin	2.56	0.51	1.94	0.48	1.47	0.28	2.32	0.44
Muscle	0.78	0.17	0.52	0.02	0.62	0.35	0.46	0.05
Bone/Marrow	1.02	0.27	0.94	0.34	0.51	0.16	0.98	0.05
Heart	2.09	0.23	2.12	0.18	1.55	0.29	1.94	0.41
Lung	3.91	0.16	3.50	0.61	1.95	0.61	2.36	0.27
Liver	8.31	2.56	8.21	0.47	8.98	1.08	7.45	0.27
Kidney	5.45	0.79	5.10	0.19	3.77	0.91	4.44	0.21
Spleen	3.44	0.50	2.70	0.11	3.48	0.68	2.64	0.43
Pancreas	1.19	0.14	1.37	0.06	1.12	0.28	1.15	0.15
Stomach	1.07	0.12	0.8	0.17	0.58	0.38	0.97	0.12
Intestine	1.96	0.17	1.41	0.15	0.99	0.33	1.15	0.39
Brain	0.17	0.02	0.13	0.04	0.08	0.03	0.16	0.03

*data is presented as percent injected activity per gram of tissue (%IA/g)

Supplemental table 3 Summary of results from the dosimetry estimation for ^{90}Y-NM600 using longitudinal ^{86}Y-NM600 PET/CT data and The Standard Mouse Model.

Target Organ	Cumulative Activity [(MBq-sec)/MBq]	$\sum_s \boldsymbol{\phi_B}(\boldsymbol{r_t} \leftarrow \boldsymbol{r_s})(\widetilde{\boldsymbol{A}}_s)$	Absorbed Dose (Gy/MBq)	Dose (9.25 MBq)
Liver	28644.57	21282.91	3.04	28.1
Spleen	1332.53	1044.35	1.74	16.1
Kidney	3980.59	3058.51	1.73	16.0
Lungs	1361.76	3344.07	3.34	30.9
Heart	1943.09	1451.62	1.89	17.5
Stomach	1588.72	2322.27	1.99	18.4
S bowel	7970.82	10947.58	1.87	17.3
L bowel	3014.02	2799.23	1.26	11.7
Thyroid	953.23	963.16	1.37	12.7
Tumor	26004.45	17978.74	2.69	24.9
Pancreas	953.23	662.53	0.95	8.7
Bone	998.62	1041.73	1.42	13.1
Marrow	30.80	47.16	0.79	7.3
Carcass	191699.11	194828.76	1.38	12.8

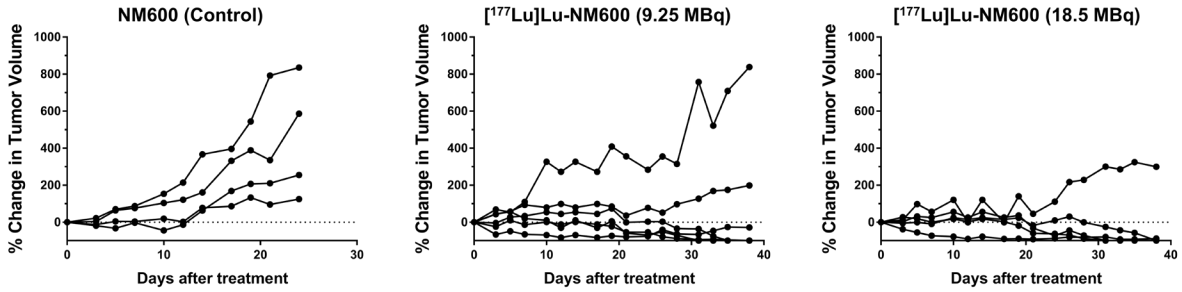

Supplemental figure 3 Individual weight of mice bearing s.c. 4T07 tumors injected with unlabeled NM600, or 9.25 or 18.5 MBq of ^{90}Y-NM600. Data are presents as percent of the initial weight.

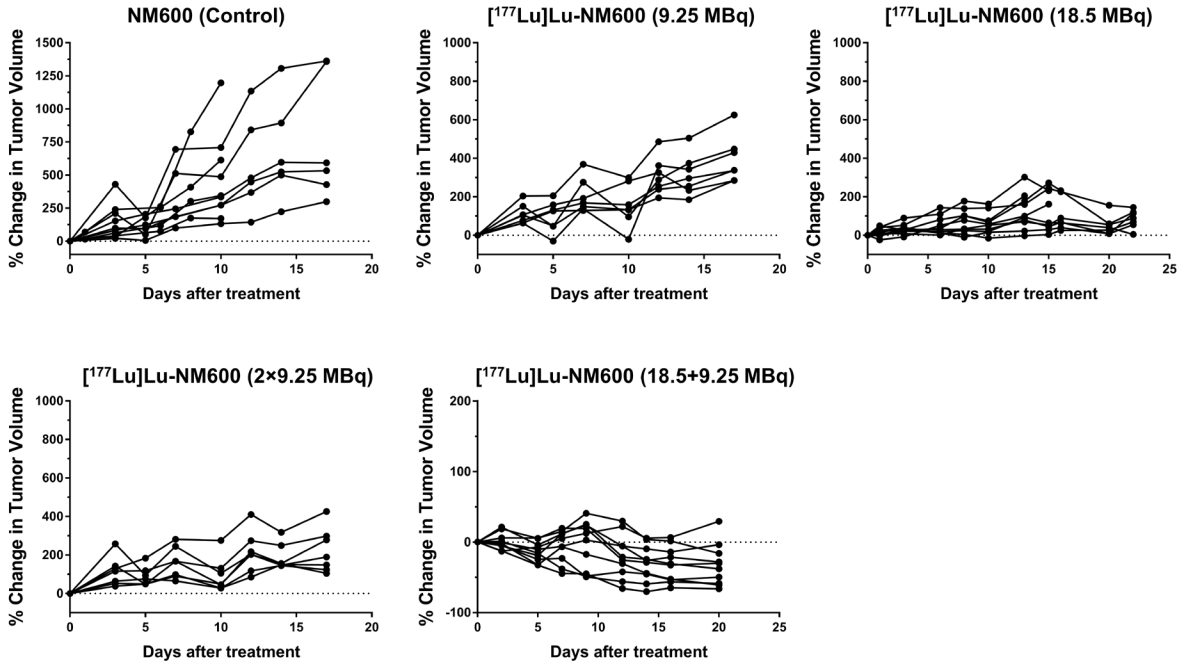

Supplemental figure 4 Individual tumor growth curves of mice bearing s.c. 4T1 tumors injected with unlabeled NM600, 9.25, 18.5, 2×9.25, or 18.5 + 9.25 MBq of ^{177}Lu-NM600. Data are presented as a fraction of the initial tumor volume.